Scientific Research Publishing

International Journal of Astronomy and Astrophysics, 2026, 16(2), 126-144
https://www.scirp.org/journal/ijaa
ISSN Online: 2161-4725
ISSN Print: 2161-4717

Transport in Astrophysics: IX. Planck's versus Callendar's Distributions

Lorenzo Zaninetti

Department of Physics, University of Turin, Turin, Italy
Email: l.zaninetti@alice.it

How to cite this paper: Zaninetti, L. (2026) Transport in Astrophysics: IX. Planck's versus Callendar's Distributions. *International Journal of Astronomy and Astrophysics*, **16**, 126-144.
https://doi.org/10.4236/ijaa.2026.162009

Received: April 28, 2026
Accepted: June 26, 2026
Published: June 29, 2026

Abstract

We compare Planck's distribution for spectral radiation with Callendar's. We cover the two regimes of wavelengths and frequencies. In each of the four cases we evaluate the dependence of the spectral radiance on the temperature for the maximum, the standard deviation and the distance between the two inflection points. The astrophysical comparison of Planck's and Callendar's distributions covers the temperature of the sun, the temperature of the cosmic microwave background, the (B-V) color and the bolometric correction.

Keywords

Stars, Atmospheres, Radiation Mechanisms, General, Blackbody Radiation

1. Introduction

The theory of spectral radiation started with Planck in 1900 [1]. Some years later, Callendar, in 1913 and 1914, proposed a different distribution for spectral radiation [2] [3]. We now briefly introduce some details of the derivation of the above distribution. We have two components: the first is due to the pressure, p, of the medium emitting the radiation,

$$p = \frac{C_1 \nu^2 (T) \mathrm{e}^{-\frac{C_2 \nu}{cT}}}{c^3}, \tag{1}$$

where C_1 is a constant, C_2 is another constant, c is the speed of light, T is the equivalent brightness temperature and ν is the considered frequency. The second part is due to the intrinsic energy $\frac{E}{\nu}$ of the photon gas:

$$\frac{E}{\nu} = \frac{C_1 C_2 \nu^3 \mathrm{e}^{-\frac{C_2 \nu}{T}}}{c^3}, \tag{2}$$

During the following years, Callendar's distribution was forgotten and Planck's distribution became the standard reference for the spectral radiation. After one hundred of years of oblivion, comparisons between the two distributions was revitalized by Tran in 2020 [4] and by Hernandez in 2025 [5]. In order to explore the differences between the two distributions in astrophysics, the following topics will be analyzed. The frequency and wavelength versions of Planck's distribution will be analyzed in Section 2, and those of the Callendar's distribution in Section 3. A comparison, in an astrophysical environment, of the two distributions will be made in Section 4.

2. Planck's Distribution

In the following we will use SI units. Table 1 presents the numerical values of the constants here used.

The percent error, δ, is defined as

$$\delta = 100 \times \left| \frac{v - v_{approx}}{v} \right|, \tag{3}$$

where v is the exact value and v_{approx} the approximate one.

Table 1. Adopted parameters.

name	value	units	Reference
speed of light	$c = 299792458$	m s^{-1}	[6]
Planck's constant	$h = 6.62607015 \times 10^{-34}$	J Hz^{-1}	[6]
Boltzmann's constant	$k = 1.380649 \times 10^{-23}$	J K^{-1}	[6]
Stefan–Boltzmann constant	$\sigma = 5.670374419 \times 10^{-8}$	W m^{-2} K^{-4}	[6]
Wien's displacement constant	$b = 0.00289777$	m K	[6]
Callendar's C_2	$C_2 = 0.013991680709$	m K	[4]
Sun's surface temperature	$T_\odot = 5772$	K	[7]
CMB temperature	$T_{CMB} = 2.72548$	K	[8]

2.1. Planck's Distribution in Frequency

The current form for the spectral energy density of Planck's distribution as a function of the frequency, ν, is

$$u_\nu(\nu, T) = \frac{8h\nu^3\pi}{c^3\left(e^{\frac{h\nu}{kT}} - 1\right)}, \tag{4}$$

where c is the speed of light, k the Boltzmann constant, T the equivalent brightness temperature and ν the considered frequency, see Equation (275) in [9], or formula (3.49) in [10]. The spectral radiance, $B_\nu(\nu, T)$, is connected with the spectral energy density through

$$B_\nu(\nu, T) = u_\nu(\nu, T)\frac{c}{4\pi}, \tag{5}$$

and therefore

$$B_\nu(\nu,T)=\frac{2h\nu^3}{c^2\left(\mathrm{e}^{\frac{h\nu}{kT}}-1\right)}\,\mathrm{W}\cdot\mathrm{sr}^{-1}\cdot\mathrm{m}^{-2}\cdot\mathrm{Hz}^{-1}, \tag{6}$$

see Equation (1.51) in [11] or formula (2.86) in [12]. According to the Stefan–Boltzmann law [13] [14] the integral of the spectral radiance in spherical coordinates is

$$\int_0^\infty B_\nu(\nu,T)\,\mathrm{d}\nu\int_0^{\frac{\pi}{2}}\cos(\theta)\sin(\theta)\,\mathrm{d}\theta\int_0^{2\pi}\mathrm{d}\phi=\sigma T^4, \tag{7}$$

where θ is the polar angle, ϕ is the azimuthal angle and the Stefan–Boltzmann constant is

$$\sigma=\frac{2k^4\pi^5}{15h^3c^2}. \tag{8}$$

The position of the peak in frequencies, ν_{peak}, can be found solving the following equation

$$\frac{\partial B_\nu(\nu,T)}{\partial\nu}=\frac{6h\nu^2}{c^2\left(\mathrm{e}^{\frac{h\nu}{kT}}-1\right)}-\frac{2h^2\nu^3\mathrm{e}^{\frac{h\nu}{kT}}}{c^2\left(\mathrm{e}^{\frac{h\nu}{kT}}-1\right)^2kT}=0, \tag{9}$$

which has the solution

$$\nu_{peak}=\frac{kT\left(W\left(-3\mathrm{e}^{-3}\right)+3\right)}{h}=\frac{2.82143kT}{h}=5.87892\times10^{10}\ \mathrm{THz}, \tag{10}$$

where W is the Lambert function, after [15] [16]. Another interesting quantity is the standard deviation in frequency

$$\Delta\nu=\sqrt{\overline{x^2}-\overline{x}^2}. \tag{11}$$

The present form of the spectral radiance is not normalized to one and therefore the moment of order m can be evaluated in the following way

$$\overline{\nu^m}=\frac{\int_0^\infty\nu^m B_\nu(\nu,T)\,\mathrm{d}\nu}{\int_0^\infty B_\nu(\nu,T)\,\mathrm{d}\nu}. \tag{12}$$

The resulting standard deviation for the Planck distribution in frequency is

$$\begin{aligned}\Delta\nu&=\frac{2\sqrt{210}Tk\sqrt{-68040\zeta(5)^2+\pi^{10}}}{21h\pi^4}\\&=\frac{2.028118240kT}{h}=4.22591\times10^{10}T\ \mathrm{Hz},\end{aligned} \tag{13}$$

where $\zeta(z)$ is the Riemann zeta function, see also Equation (12) in [17] which gives the same result. The positions of the inflection points are given by the solutions of the following transcendental equation

$$\frac{\partial^2 B_\nu(\nu,T)}{\partial \nu^2} = \frac{12h\nu}{c^2\left(e^{\frac{h\nu}{kT}}-1\right)} - \frac{12h^2\nu^2 e^{\frac{h\nu}{kT}}}{c^2\left(e^{\frac{h\nu}{kT}}-1\right)^2 kT} + \frac{4h^3\nu^3\left(e^{\frac{h\nu}{kT}}\right)^2}{c^2\left(e^{\frac{h\nu}{kT}}-1\right)^3 k^2T^2} - \frac{2h^3\nu^3 e^{\frac{h\nu}{kT}}}{c^2\left(e^{\frac{h\nu}{kT}}-1\right)^2 k^2T^2} = 0. \tag{14}$$

In order to derive two semi-analytical results, we replace the above equation with a Padé approximant of order $[2,2]$

$$\frac{\partial^2 B_\nu(\nu,T)}{\partial \nu^2} \approx \frac{96k^3T^3 - 132T^2hk^2\nu + 34Th^2k\nu^2}{24c^2k^2T^2 + 3Tc^2hk\nu + c^2h^2\nu^2} = 0. \tag{15}$$

The two approximate solutions, ν_{lower} and ν_{upper} are

$$\nu_{lower} \approx \frac{2\left(\frac{33}{34} - \frac{\sqrt{273}}{34}\right)Tk}{h}, \tag{16}$$

ν_{upper} and

$$\nu_{upper} \approx \frac{2\left(\frac{33}{34} + \frac{\sqrt{273}}{34}\right)Tk}{h}. \tag{17}$$

The percent error of the previous two solutions at the temperature of the sun, see Table 1, is 0.3088% for the lower solution and 36.99% for the upper solution. The distance between the two approximate solutions is

$$\nu_{upper} - \nu_{lower} \approx \frac{1.94384kT}{h} = 4.05032\times10^{10}T \text{ Hz}. \tag{18}$$

When $\frac{h\nu}{kT} \ll 1$ is the Taylor expansion to the fourth order, we obtain

$$B_\nu(\nu,T) \approx \frac{2kT\nu^2}{c^2}, \tag{19}$$

which is called the Rayleigh-Jeans law, when instead $\frac{h\nu}{kT} \gg 1$ is an asymptotic expansion, we obtain the approximation

$$B_\nu(\nu,T) \approx \frac{2h\nu^3}{c^2 e^{\frac{h\nu}{kT}}}, \tag{20}$$

which is called Wien's law.

2.2. Planck's Distribution in Wavelength

The current form for the spectral radiance of Planck's distribution as a function

of the wavelength, λ, is

$$B_\lambda(\lambda,T)=\frac{2hc^2}{\lambda^5\left(e^{\frac{hc}{\lambda kT}}-1\right)}\,\mathrm{W}\cdot\mathrm{sr}^{-1}\cdot\mathrm{m}^{-3}, \tag{21}$$

see, for example, Equation (3.52) in [10] or formula (2.88) in [12]. In going from frequencies to wavelengths, the following differential has been used, dropping the negative sign

$$d\nu=-\frac{c}{\lambda^2}d\lambda. \tag{22}$$

The integral of the spectral radiance in polar coordinates for wavelengths is

$$\int_0^\infty B_\lambda(\lambda,T)d\lambda\int_0^{\frac{\pi}{2}}\cos(\theta)\sin(\theta)d\theta\int_0^{2\pi}d\phi=\sigma T^4. \tag{23}$$

The position of the peak in wavelength, λ_{peak}, can be found by solving the equation

$$\frac{\partial B_\lambda(\lambda,T)}{\partial\lambda}=-\frac{10hc^2}{\lambda^6\left(e^{\frac{hc}{\lambda kT}}-1\right)}+\frac{2h^2c^3e^{\frac{hc}{\lambda kT}}}{\lambda^7\left(e^{\frac{hc}{\lambda kT}}-1\right)^2kT}=0, \tag{24}$$

which has the solution

$$\lambda_{peak}=\frac{hc}{Tk\left(W\left(-5e^{-5}\right)+5\right)}=\frac{0.00289777}{T}\,\mathrm{m}. \tag{25}$$

Inserting in the above equation the temperature of the sun, see **Table 1**, we obtain

$$\lambda_{peak}=5.02039\times10^{-7}\,\mathrm{m}=502.039\,\mathrm{nm}. \tag{26}$$

The standard deviation in wavelength for the Planck distribution is evaluated as in Equation (12) once the frequency is replaced by the wavelength

$$\Delta\lambda=\frac{ch\sqrt{10\pi^6-3600\zeta(3)^2}}{2Tk\pi^4}=\frac{0.0049}{T}\,\mathrm{m}, \tag{27}$$

3. Callendar's Distribution

3.1. Callendar's Distribution in Frequency

The form for the spectral energy density of Callendar's distribution as a function of the frequency, ν, is

$$u_\nu(\nu,T)=\frac{C_1\nu^2\left(T+\frac{C_2\nu}{c}\right)e^{-\frac{C_2\nu}{cT}}}{c^3}, \tag{28}$$

where C_1 is a constant, C_2 is another constant, c is the speed of light, T is the equivalent brightness temperature and ν is the considered frequency, see Equation (6) in [4].

The spectral radiance, $B_\nu(\nu,T)$, of Callendar's distribution according to Equation (28) is

$$B_\nu(\nu,T)=\frac{C_1\nu^2\left(T+\frac{C_2\nu}{c}\right)\mathrm{e}^{-\frac{C_2\nu}{cT}}}{4c^2\pi}, \tag{29}$$

see Equation (3.121) in [5]. The integral of the spectral radiance for Callendar's distribution in spherical coordinates is

$$\int_0^\infty B_\nu(\nu,T)\,\mathrm{d}\nu\int_0^{\frac{\pi}{2}}\cos(\theta)\sin(\theta)\,\mathrm{d}\theta\int_0^{2\pi}\mathrm{d}\phi=\frac{2cC_1T^4}{C_2^3}=\sigma T^4. \tag{30}$$

The above formula allows deriving a formula for C_1 once C_2 is given:

$$C_1=\frac{\sigma C_2^3}{2c}, \tag{31}$$

which means with the data of **Table 1**

$$C_1=2.590423052\times10^{-22}. \tag{32}$$

The position of the peak in frequencies of Callendar's distribution, ν_{peak}, can be found by solving the equation

$$\begin{aligned}\frac{\partial B_\nu(\nu,T)}{\partial\nu}=&\frac{C_1\nu\left(T+\frac{C_2\nu}{c}\right)\mathrm{e}^{-\frac{C_2\nu}{cT}}}{2c^2\pi}+\frac{C_1\nu^2C_2\mathrm{e}^{-\frac{C_2\nu}{cT}}}{4c^3\pi}\\&-\frac{C_1\nu^2\left(T+\frac{C_2\nu}{c}\right)C_2\mathrm{e}^{-\frac{C_2\nu}{cT}}}{4c^3T\pi}\\=&\,0,\end{aligned} \tag{33}$$

which has the solution

$$\nu_{peak}=\frac{\left(1+\sqrt{3}\right)cT}{C_2}=2.142647936\times10^{10}\left(1+\sqrt{3}\right)T\ \text{Hz}. \tag{34}$$

The standard deviation in frequency for Callendar's distribution is evaluated following Equation (12)

$$\Delta\nu=\frac{3\sqrt{7}cT}{4C_2}. \tag{35}$$

The equation for the inflection points of Callendar's distribution is

$$\frac{\partial^2B_\nu(\nu,T)}{\partial\nu^2}=\frac{\mathrm{e}^{-\frac{C_2\nu}{cT}}C_1\left(2T^3c^3+2T^2c^2\nu C_2-5Tc\nu^2C_2^2+\nu^3C_2^3\right)}{4c^5T^2\pi}=0, \tag{36}$$

which is a third degree equation with two positive solutions and a negative solution. The lower positive solution is

$$\nu_{lower}=\frac{Tc}{C_2}, \tag{37}$$

and the upper positive solution is

$$\nu_{upper} = \frac{\left(2+\sqrt{6}\right)Tc}{C_2}. \tag{38}$$

As a consequence, the distance between the two inflection points of Callendar's distribution is

$$\nu_{upper} - \nu_{lower} = \frac{Tc\left(1+\sqrt{6}\right)}{C_2}. \tag{39}$$

When $\frac{C_2\nu}{cT} \ll 1$ is a Taylor expansion to the third order, we obtain

$$B_\nu(\nu,T) \approx \frac{C_1 T \nu^2}{4\pi c^2}, \tag{40}$$

which shares with the Rayleigh-Jeans law the ν^2 dependence.

3.2. Callendar's Distribution in Wavelength

Callendar's distribution as a function of the wavelength, λ, can be obtained using the absolute value of the differential $\mathrm{d}\nu$ given by formula (22)

$$B_\lambda(\lambda,T) = \frac{C_1\left(T+\frac{C_2}{\lambda}\right)\mathrm{e}^{-\frac{C_2}{\lambda T}}c}{4\lambda^4\pi}\,\mathrm{W}\cdot\mathrm{sr}^{-1}\cdot\mathrm{m}^{-3}. \tag{41}$$

The integral of the spectral radiance for Callendar's distribution in polar coordinates for wavelengths is

$$\int_0^\infty B_\lambda(\lambda,T)\mathrm{d}\lambda \int_0^{\frac{\pi}{2}} \cos(\theta)\sin(\theta)\mathrm{d}\theta \int_0^{2\pi} \mathrm{d}\phi = \frac{2cC_1T^4}{\pi C_2^3}. \tag{42}$$

The position of the peak in wavelength can be found by solving the equation

$$\frac{\partial B_\lambda(\lambda,T)}{\partial\lambda} = \frac{\mathrm{e}^{-\frac{C_2}{\lambda T}}C_1 c\left(-4T^2\lambda^2 - 4C_2\lambda T + C_2^2\right)}{4\lambda^7 T\pi} = 0, \tag{43}$$

which has the positive solution

$$\lambda_{peak} = \frac{\left(\sqrt{2}-1\right)C_2}{2T}. \tag{44}$$

Wien's law states that

$$\lambda_{peak} = b/T, \tag{45}$$

where b is Wien's displacement constant, see Table 1 for its numerical view. Combining the above two equations we derive a numerical value for C_2 from our formulae

$$C_2 = 0.01399168072\ \mathrm{m}\cdot\mathrm{K}, \tag{46}$$

which has a relative percent error of 7.1471×10^{-8} with respect to the value of Table 1. The standard deviation in wavelength for Callendar's distribution is evaluated as in Equation (12) once the frequency is replaced by the wavelength

$$\Delta\lambda = \frac{\sqrt{7}C_2}{8T} = \frac{0.00462731}{T}\text{m}. \tag{47}$$

The positions of the inflection points are given by the solutions of the following cubic equation

$$\frac{\partial^2 B_\lambda(\lambda,T)}{\partial\lambda^2} = \frac{e^{-\frac{C_2}{\lambda T}} C_1 c\left(20T^3\lambda^3 + 20T^2\lambda^2 C_2 - 11T\lambda C_2^2 + C_2^3\right)}{4\lambda^9 T^2 \pi} = 0. \tag{48}$$

There are three roots:

$$\frac{\left(\left(-4150+45\text{I}\sqrt{685}\right)^{2/3} - 10\left(-4150+45\text{I}\sqrt{685}\right)^{1/3} + 265\right)C_2}{30\left(-4150+45\text{I}\sqrt{685}\right)^{1/3} T}, \tag{49a}$$

$$-\frac{\left(\sqrt{265}\cos\left(\frac{\arctan\left(\frac{9\sqrt{685}}{830}\right)}{3}+\frac{\pi}{6}\right)\sqrt{3}+\sqrt{265}\sin\left(\frac{\arctan\left(\frac{9\sqrt{685}}{830}\right)}{3}+\frac{\pi}{6}\right)+10\right)C_2}{30T}, \tag{49b}$$

$$\frac{\left(\sqrt{265}\cos\left(\frac{\arctan\left(\frac{9\sqrt{685}}{830}\right)}{3}+\frac{\pi}{6}\right)\sqrt{3}-\sqrt{265}\sin\left(\frac{\arctan\left(\frac{9\sqrt{685}}{830}\right)}{3}+\frac{\pi}{6}\right)-10\right)C_2}{30T}. \tag{49c}$$

The negative real root is Equation (49b) and the two complex conjugate roots are Equation (49a) and Equation (49c). The distance between the two inflection points is real:

$$\lambda_{upper} - \lambda_{lower} = \frac{0.1730190589C_2}{T}. \tag{50}$$

4. Astrophysical Applications

We will now evaluate the χ^2 statistic

$$\chi^2 = \sum_{i=1}^{n}\left(y_i - ytheo_i\right)^2, \tag{51}$$

where y_i is the ith element of the sample, $ytheo_i$ is the ith theoretical element and n the number of elements of the sample.

4.1. The Temperature of the Sun

The solar spectrum at the top of the atmosphere, e.g., at 35 km, is called air mass zero (AM0) [18]. We fit the AM0 data with the function

$$f(\lambda,T)=A\times B_{\lambda}(\lambda,T), \tag{52}$$

where B can be either Planck's or Callendar's spectral radiance and A is a constant which allows matching the data. We can find the temperature both with an exact method and with an approximate method:

1) The temperature and the constant can be found through the Levenberg–Marquardt method (subroutine MRQMIN in [19]), see Equation (52).

2) The temperature can be found from the wavelength corresponding to the peak, see Equation (25) for the Planck case and Equation (44) for the Callendar case.

3) The temperature can be found from the standard deviation, see Equation (27) for the Planck case and Equation (35) for the Callendar case.

The numerical results are presented in **Table 2**. A graphical display of the two distributions is presented in **Figure 1** for the Planck distribution and **Figure 2** for the Callendar distribution.

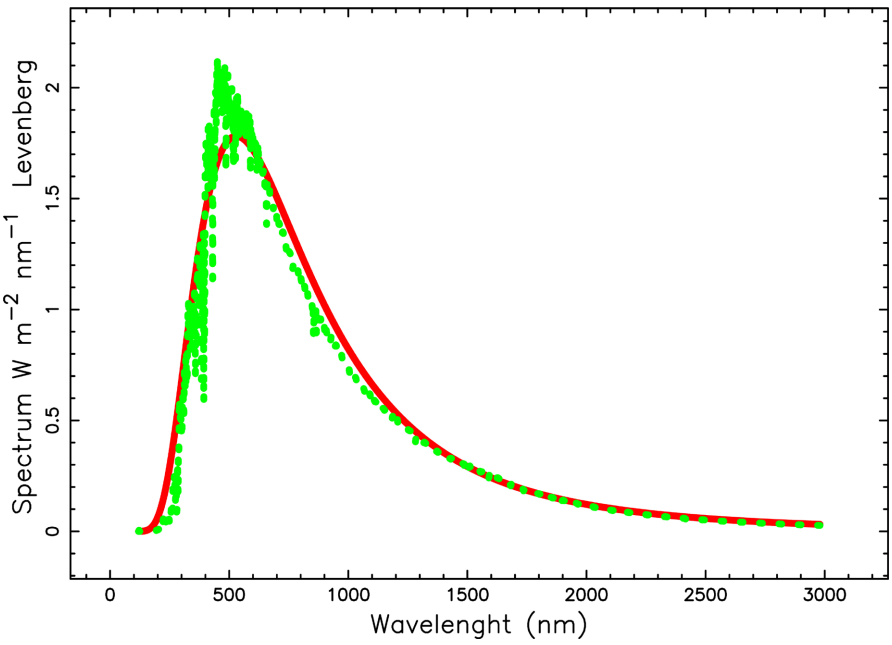

Figure 1. Spectral radiance versus wavelength in nm for AM0, green points, and theoretical fit for the Planck distribution, red line.

Table 2. Fitting AM0.

distribution	Method	$T(\mathrm{K})$	A	percent error
Planck	Levenberg	5467.49	8.9×10^{-14}	5.27%

Continued

Planck	maximum	6432.34		11.44%
Planck	std. dev.	6591.60		14.19%
Callendar	Levenberg	5325.09	2.64347×10^{-35}	7.74%
Callendar	maximum	6432.34		11.44%
Callendar	std. dev.	6217.75		7.72%

4.2. Cosmic Microwave Background

The cosmic microwave background (CMB) is a spectral energy density measured outside the atmosphere that presents a thermal behavior. The spectral energy density and the spectral radiance differ by a constant factor, see Equation (5). The data of the COBE/FIRAS CMB monopole spectrum [20] are available on line, see the Acknowledgments.

1) Also in this case the temperature and the constant can be found through the Levenberg–Marquardt method, see Equation (4).

2) The temperature can be found from the frequency corresponding to the peak, see Equation (10) for the Planck case and Equation (34) for the Callendar case.

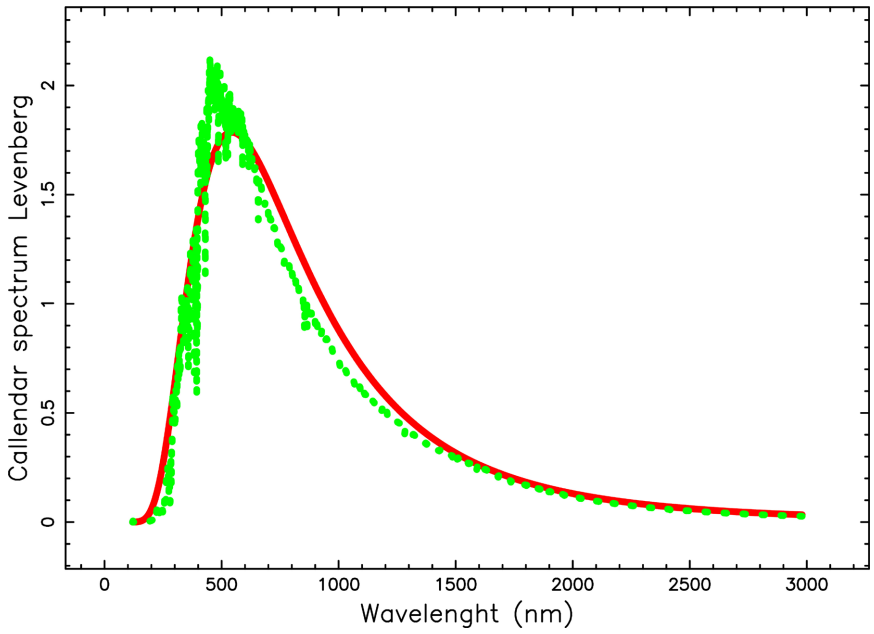

Figure 2. Spectral radiance versus wavelength in nm for AM0, green points, and theoretical fit for the Callendar distribution, red line.

The numerical results are presented in **Table 3**. A graphical display of the two distributions is presented in **Figure 3** for the Planck distribution and **Figure 4** for the Callendar distribution. The relative percent error between the Planck's distribution and the Callendar's distribution in presented in **Figure 5**: briefly, we can say, according to Tran (2020) [4], that the two distributions are indistinguishable.

Table 3. Fitting COBE/FIRAS CMB monopole spectrum.

distribution	Method	$T(\mathrm{K})$	A	Percent error
Planck	Levenberg	2.72500873	9.99974247×10^{19}	$1.72943305\times10^{-2}\%$
Planck	maximum	2.77919626		1.97088885%
Callendar	Levenberg	2.72385907	618341.5	$5.94760515\times10^{-2}\%$
Callendar	maximum	2.79111409		2.40816355%

4.3. Planck's Color System

The brightness of the radiation from a Planck distribution in wavelengths is given by Equation (21). The color-difference, (C_1-C_2), can be expressed as

$$(C_1-C_2)=m_1-m_2=K-2.5\log_{10}\frac{\int S_1 I_\lambda \mathrm{d}\lambda}{\int S_2 I_\lambda \mathrm{d}\lambda}, \tag{53}$$

where S_λ is the sensitivity function in the region specified by the index λ, K is a constant and I_λ is the energy flux reaching the earth. We now define a sensitivity function for a pseudo-monochromatic system

$$S_\lambda=\delta(\lambda-\lambda_i) \quad i=U,B,V,R,I, \tag{54}$$

where δ denotes the Dirac delta function. In this pseudo-monochromatic color system the color-difference is

$$(C_1-C_2)=K-2.5\log_{10}\frac{\lambda_2^5}{\lambda_1^5}\frac{\left(\exp\left(\frac{hc}{\lambda_2 kT}\right)-1\right)}{\left(\exp\left(\frac{hc}{\lambda_1 kT}\right)-1\right)}, \tag{55}$$

where the wavelengths λ_1 and λ_2 are those of colors C_1 and C_2.

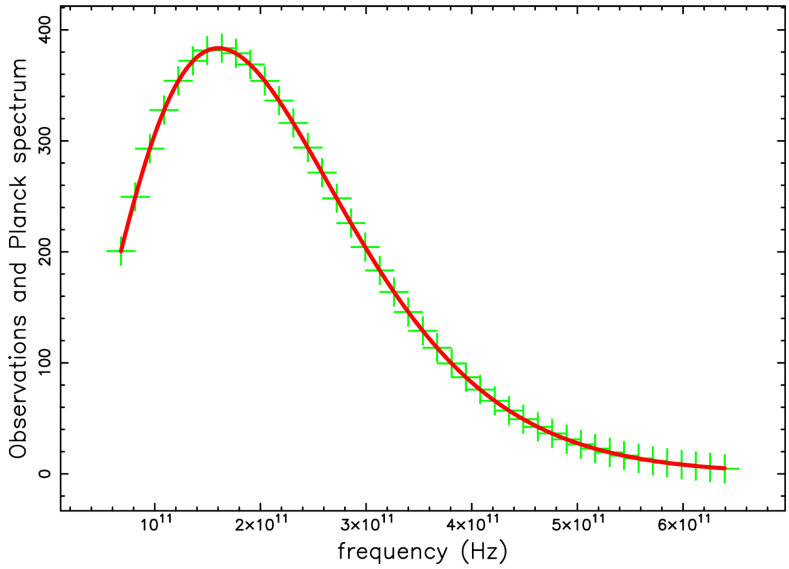

Figure 3. Spectral radiance versus frequency in Hz for FIRAS data, green points, and theoretical fit for the Planck distribution, red line.

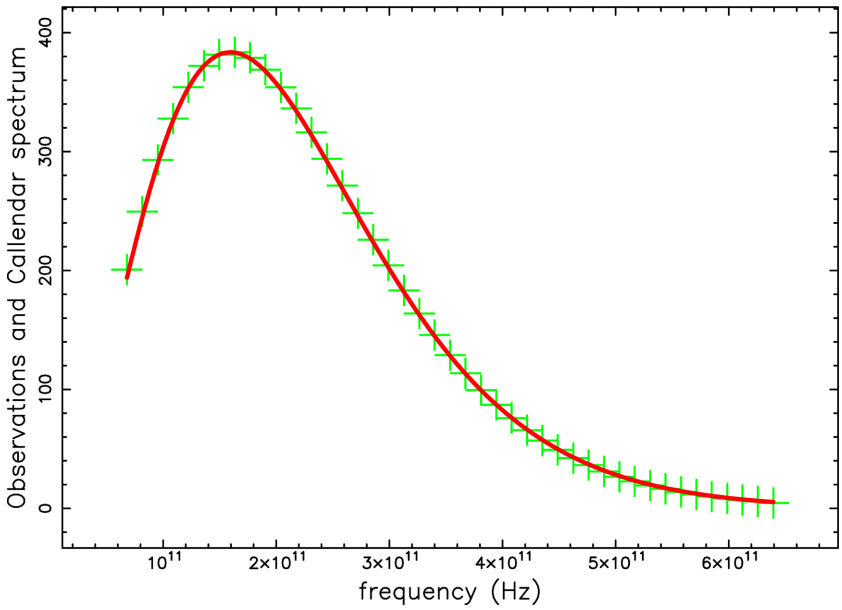

Figure 4. Spectral radiance versus frequency in Hz for FIRAS data, green points, and theoretical fit for the Callendar distribution, red line.

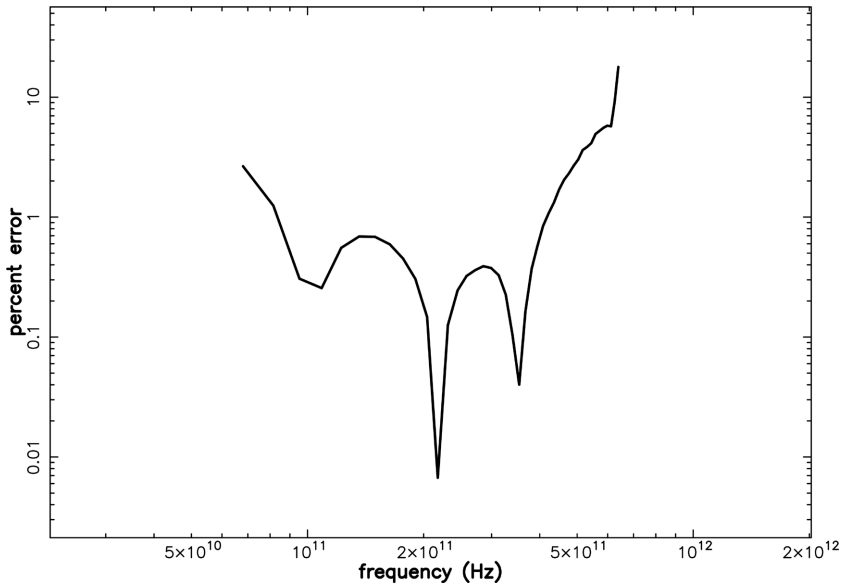

Figure 5. Relative percent error versus frequency in Hz for FIRAS data between Planck distribution, the true value, and Callendar distribution, the measured value.

Table 4. Johnson system.

symbol	wavelength (Å)
U	3600
B	4400
V	5500
R	7100
I	9700

The previous expression for the color can be expanded in a Taylor series about the point $T=\infty$. When the order of the expansion is 2, we have

$$\left(C_1-C_2\right)_{app}=-\frac{5}{2}\ln\left(\frac{\lambda_2^{\,4}}{\lambda_1^{\,4}}\right)\frac{1}{\ln(10)}-\frac{5}{4}\frac{hc\left(\lambda_1-\lambda_2\right)}{\lambda_2\lambda_1 k\ln(10)T}-\frac{5}{48}\frac{h^2c^2\left(\lambda_1^{\,2}-\lambda_2^{\,2}\right)}{\lambda_2^{\,2}\lambda_1^{\,2}k^2\ln(10)T^2}, \tag{56}$$

where the index *app* means approximated. We now continue inserting the value of the physical constants as given by CODATA [21] and the wavelength of the color as given by Table 15.6 in [22] and visible in **Table 4**. Another important step is the calibration of the color on the maximum temperature T_{cal} of the reference tables. For example, for MAIN SEQUENCE V at $T_{cal}=42000$, see Table 15.7 in [22], $\left(B-V\right)=-0.3$ and therefore a constant should be added to formula (58) in order to obtain such a value. With these recipes we obtain, for example

$$\left(B-V\right)=-0.4243+\frac{3543}{T}+\frac{17480000}{T^2} \tag{57}$$

MAIN SEQUENCE, V when $-0.33<\left(B-V\right)<1.64$.
More details can be found in [23].

4.4. Callendar's Color System

In the pseudo-monochromatic color system, the color-difference for Callendar's distribution is

$$\left(C_1-C_2\right)=-\frac{5\ln\left(\frac{\left(T+\frac{C_2}{\lambda_1}\right)\mathrm{e}^{-\frac{C_2}{\lambda_1 T}}\lambda_2^4}{\lambda_1^4\left(T+\frac{C_2}{\lambda_2}\right)\mathrm{e}^{-\frac{C_2}{\lambda_2 T}}}\right)}{2\ln(10)}, \tag{58}$$

where the wavelengths λ_1 and λ_2 are those of the colors C_1 and C_2. **Figure 6** displays the (B-V) color as a function of the temperature for the Planck distribution as given by Equation (55) and the corresponding value for Callendar's distribution, see Equation (58).

In the absence of a reliable Taylor series such as that given by Equation (56), we present a quadratic regression in the variable $\frac{1}{T}$ for the Callendar distribution

$$\left(B-V\right)=-0.7657659+\frac{8489.875}{T}-\frac{628398.4}{T^2} \tag{59}$$

MAIN SEQUENCE, V when $-0.33<\left(B-V\right)<1.64$,
which is displayed in **Figure 7**.

A comparison between the two distributions is presented in **Table 5**.

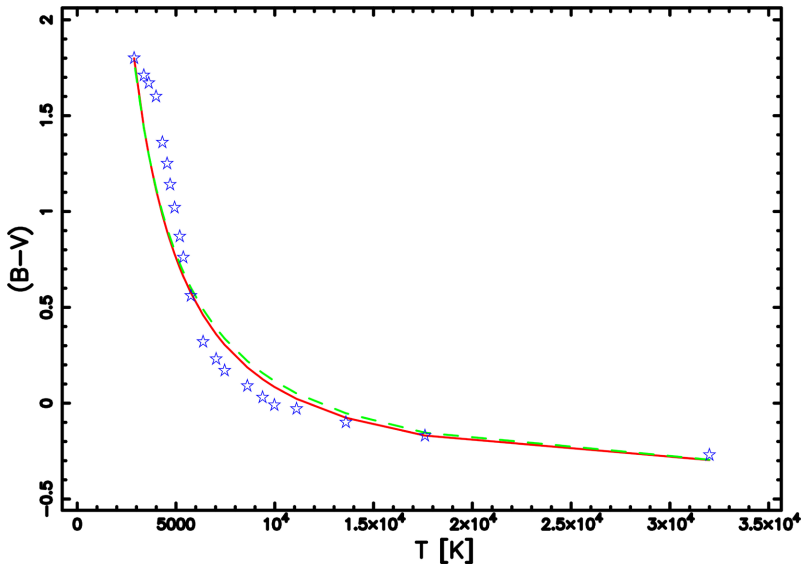

Figure 6. B-V versus temperature. The red full line is for Planck's distribution and the green dashed line for Callendar's. The calibrated data extracted from Table 15.7 in [22] are shown as empty blue stars.

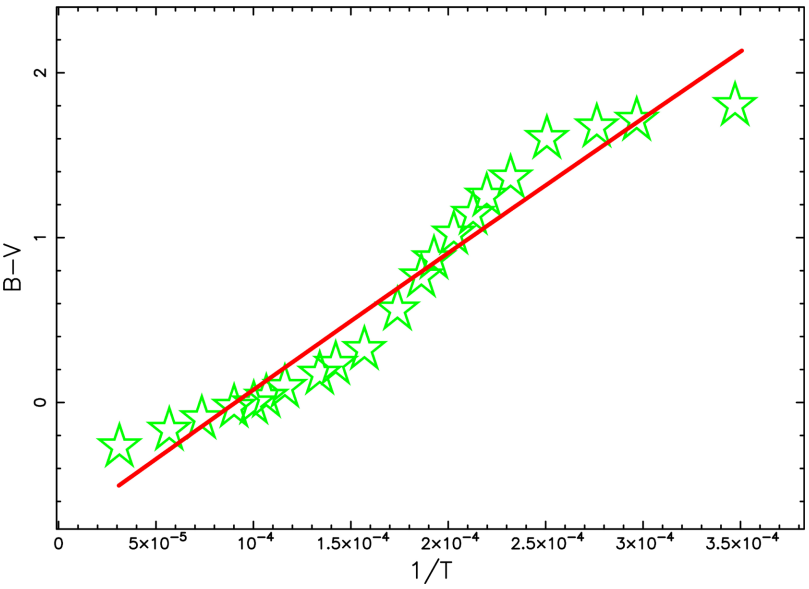

Figure 7. B-V versus a quadratic model in 1 T for the Callendar distribution, red line and astronomical points, green empty stars.

Table 5. B-V results.

distribution	Formula	χ^2
Planck	(55)	0.983
Callendar	(58)	0.985

4.5. Bolometric Correction for Planck's Distribution

The bolometric correction, BC, defined as always negative, is

$$BC = M_{\text{bol}} - M_V, \tag{60}$$

where M_{bol} is the absolute bolometric magnitude and M_V is the absolute visual magnitude. It can be expressed as

$$BC = \frac{5}{2}\frac{\ln\left(15\left(\frac{hc}{kT\pi}\right)^4\left(\frac{1}{\lambda_V}\right)^5\frac{1}{\exp\left(\frac{hc}{kT\lambda_V}\right)-1}\right)}{\ln(10)} + K_{BC}, \tag{61}$$

where λ_V is the visual wavelength and K_{BC} a constant. We now expand in a Taylor series about the point $T = \infty$

$$BC_{app} = -\frac{15}{2}\frac{\ln(T)}{\ln(10)} - \frac{5}{4}\frac{hc}{k\lambda_V \ln(10) T} - \frac{5}{48}\frac{h^2c^2}{k^2\lambda_V^2 \ln(10) T^2} + K_{BC}. \tag{62}$$

The constant K_{BC} can be found with the following procedure. The maximum of BC_{app} is at $T_{\max}$, where the index max stands for maximum

$$T_{\max} = \frac{1}{6}\frac{\left(\frac{\sqrt{5}}{2}+\frac{1}{2}\right)ch}{k\lambda_V}. \tag{63}$$

Given the fact that the observed maximum for the BC is −0.09 at 7300 K in the case of MAIN SEQUENCE V we easily compute K_{BC} and the following approximate result is obtained

$$BC_{app} = 31.41 - 3.257\ln(T) - \frac{14200}{T} - \frac{3.09610^7}{T^2}. \tag{64}$$

Figure 8 presents the exact and the approximate values of BC as well as the calibrated data.

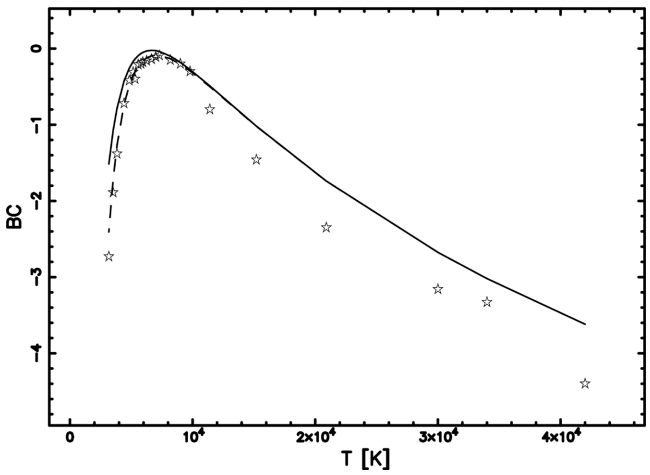

Figure 8. Exact BC as deduced from the Planck distribution, or Equation (61), traced with a full line. Approximate BC as deduced from the Taylor expansion, or Equation (64), traced with a dashed line. The calibrated data for MAIN SEQUENCE V are extracted from Table 15.7 in Cox (2000) and are represented through empty stars.

4.6. Bolometric Correction for Callendar's Distribution

The bolometric correction of Callendar's distribution for a color characterized by a wavelength λ_1 is

$$BC = \frac{5 \ln\left(\frac{\left(T + \frac{C_2}{\lambda_1} \right) e^{-\frac{C_2}{\lambda_1 T}} C_2^3}{8 \lambda_1^4 T^4} \right)}{2 \ln(10)}. \tag{65}$$

The maximum in temperature, $T_{\max}$, of the bolometric correction is easily found by setting to zero the first derivative of the above equation and solving for T

$$T_{\max} = \frac{\left(-\frac{1}{2} + \frac{\sqrt{21}}{6} \right) C_2}{\lambda_1}, \tag{66}$$

which for the V band is $T_{\max} = 6709.96$ K . Figure 9 displays the bolometric correction in the visual band for the Callendar and Planck distributions as well the calibrated data.

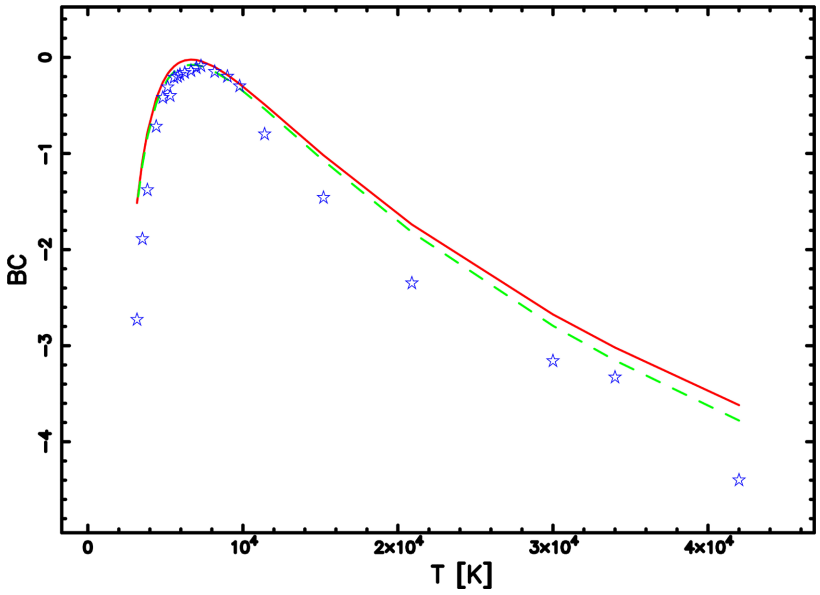

Figure 9. *BC* in the V band versus temperature for Callendar's distribution, green dashed line, Planck's distribution, red line, and calibrated data, blue empty stars.

A comparison between the two distributions is presented in Table 6.

Table 6. *BC* results.

distribution	Formula	χ^2
Planck	(61)	4.39
Callendar	(65)	3.5

5. Conclusions

5.1. Analytical Results

We considered two distributions for the spectral radiance: one introduced by Planck and the other by Callendar, in the two regimes of wavelengths and frequencies. In these four cases we computed the dependence of the spectral radiance on the temperature for the maximum, the standard deviation evaluated with the technique of the probability distributions which are normalized to one and the distance between the two inflection points. This paper relies mainly on curve fitting and empirical comparisons. The physical justification and astrophysical implications of using Callendar's distribution instead of Planck's distribution is demanded to future efforts.

5.2. Application to the Solar Spectrum

The difference in the evaluation of the solar spectrum can be expressed as a percent error with respect to the quoted temperature of the sun. The Levenberg method gives a percent error of 5.27% for Planck's distribution against 7.74% for Callendar's distribution, see **Table 2**. In other words, the determination of the correct temperature of the sun may depends on the chosen model; as an example [24] processed seven different models, finding the range of values $5400 < T < 6400$.

5.3. Application to the CMB

The Levenberg method gives a percent error of $1.72943305\times10^{-2}\%$ for Planck's distribution against $5.94760515\times10^{-2}\%$ for Callendar's distribution, with respect to the quoted temperature of the CMB, see **Table 1**. This means, according to [4], that the two distributions are "indistinguishable."

5.4. Application to B-V

For the B-V color, the value of χ^2 is 0.983 for the Planck distribution and 0.985 for the Callendar distribution, see **Table 5**, which means that the two distributions are indistinguishable.

5.5. Application to *BC*

In the case of the bolometric correction, the value of χ^2 is 4.39 for the Planck distribution and 3.5 for the Callendar distribution, see **Table 6**, which means that the Callendar distribution produces a better fit than does the Planck distribution.

Acknowledgements

The data on the CMB monopole spectrum are available at the following WWW address
https://lambda.gsfc.nasa.gov/data/cobe/firas/monopole_spec/firas_monopole_spec_v1.txt.

Conflicts of Interest

The author declares no conflicts of interest regarding the publication of this paper.

References

[1] Planck, M. (1900) On the Theory of the Energy Distribution Law of the Normal Spectrum. *Verhandlungen der Deutschen Physikalischen Gesellschaft*, **2**, 237-245.

[2] Callendar, H.L. (1913) LXVI. *Note on Radiation and Specific Heat. The London, Edinburgh, and Dublin Philosophical Magazine and Journal of Science*, **26**, 787-791. https://doi.org/10.1080/14786441308635023

[3] Callendar, H.L. (1914) XCVI. *Thermodynamics of Radiation. The London, Edinburgh, and Dublin Philosophical Magazine and Journal of Science*, **27**, 870-880. https://doi.org/10.1080/14786440508635158

[4] Tran, M. (2020) Planck's and Callendar's Blackbody Radiation Formulas and Their Fitness to Experimental Data. *European Journal of Physics*, **41**, Article 025102. https://doi.org/10.1088/1361-6404/ab513b

[5] Hernandez, H. (2025) Modelling Thermal Radiation 3. Spectral Radiation, Fors Chem Research Reports, 1-17

[6] Mohr, P.J., Newell, D.B., Taylor, B.N. and Tiesinga, E. (2025) CODATA Recommended Values of the Fundamental Physical Constants: 2022. *Reviews of Modern Physics*, **97**, Article No. 025002. https://doi.org/10.1103/revmodphys.97.025002

[7] Phillips, K.J.H. (1995) Guide to the Sun. Cambridge University Press.

[8] Fixsen, D.J. (2009) The Temperature of the Cosmic Microwave Background. *The Astrophysical Journal*, **707**, 916-920. https://doi.org/10.1088/0004-637x/707/2/916

[9] Planck, M. (1959) The Theory of Heat Radiation. Dover Publications.

[10] Kraus, J.D. (1986) Radio Astronomy. Cygnus-Quasar Books.

[11] Rybicki, G. and Lightman, A. (1991) Radiative Processes in Astrophysics. Wiley-Interscience.

[12] Condon, J.J. and Ransom, S.M. (2016) Essential Radio Astronomy. Princeton University Press.

[13] Stefan, J. (1879) Über die beziehung der wärmestrahlungund der temperature. Sitzungs-berichte der KaiserlichenAkademie der Wissenschaften, Mathe-matische-Naturwissenschaftliche Classe Abteilung II, Vol. 79, 391-428.

[14] Boltzmann, L. (1884) Ableitung des stefan'schen gesetzes, betreffend die abhängigkeit der wärmestrahlung von der temperatur aus der electromagnetischen lichttheorie. *Annalen der Physik*, **258**, 291-294. https://doi.org/10.1002/andp.18842580616

[15] Lambert, J.H. (1758) Observations variae in mathesin puram, *Acta Helvitica*, **3**, 128-168.

[16] Olver, F.W.J., Lozier, D.W., Boisvert, R.F. and Clark, C.W. (2010) NIST Handbook of Mathematical Functions. Cambridge University Press.

[17] Reed, B.C. (2025) Characterizing the Breadth of the Planck Function. *American Journal of Physics*, **93**, 1000-1004. https://doi.org/10.1119/5.0281796

[18] Xu, G., Ke, Z., Zhuang, C., Li, Y., Cai, R., Yang, Y., *et al.* (2023) Measurements and Analysis of Solar Spectrum in near Space. *Energy Reports*, **9**, 1764-1773. https://doi.org/10.1016/j.egyr.2023.04.229

[19] Press, W.H., Teukolsky, S.A., Vetterling, W.T. and Flannery, B.P. (1992) Numerical

Recipes in FORTRAN. The Art of Scientific Computing, Cambridge University Press.

[20] Fixsen, D.J. and Mather, J.C. (2002) The Spectral Results of the Far-Infrared Absolute Spectrophotometer Instrument on *Cobe*. *The Astrophysical Journal*, **581**, 817-822. https://doi.org/10.1086/344402

[21] Mohr, P.J. and Taylor, B.N. (2005) CODATA Recommended Values of the Fundamental Physical Constants: 2002. *Reviews of Modern Physics*, **77**, 1-107. https://doi.org/10.1103/revmodphys.77.1

[22] Cox, A.N. (2000) Allen's Astrophysical Quantities. Springer.

[23] Zaninetti, L. (2008) Semi-Analytical Formulas for the Hertzsprung-Russell Diagram. *Serbian Astronomical Journal*, **177**, 73-85. https://doi.org/10.2298/saj0877073z

[24] Hernandez, H. (2026) Analysis of the am0 Spectrum of Solar Radiation. *ForsChem Research Reports*, **11**, 1-13.